FORMATION OF CEREOUS SULPHATE PHASE UPON INTERACTION OF SO₂ WITH CERIA AT ROOM TEMPERATURE
Thermal analysis, Raman and EPR study

R. Flouty, E. Abi-Aad, S. Siffert and A. Aboukaïs[*]

Laboratoire de Catalyse et Environnement E.A. 2598, MREID, Université du Littoral Côte d'Opale, MREID 145 avenue Maurice Schumann, 59140 Dunkerque, France

Abstract

The adsorption of SO₂ gas on ceria solid at room temperature has been investigated by thermal analysis, Raman spectroscopy and electron paramagnetic resonance (EPR). The results confirm that SO₂ transformation into sulphate species occurs at 25°C with a concomitant reduction of Ce^{4+} to Ce^{3+} ions. The formation of Ce(III)-sulphate phase has been evidenced on ceria surface. The thermal analysis revealed a complete decomposition of cereous sulphate phase to CeO₂ at 785°C. The change of oxidation state of Ce(IV) to Ce(III) during the formation of sulphate phase has been confirmed also by EPR technique.

Keywords: CeO₂, cereous sulphate formation, EPR, Raman, SO₂ adsorption, thermal analysis

Introduction

Ceria had received considerable attention in recent years mainly due to its presence in fluid catalytic cracking (FCC) [1] and three-way catalyst systems (TWC) [2]. This oxide was first added to automobile exhaust gas treatment catalysts for its oxygen storage capacities (OSC) but, in practice, the role of cerium oxide has been shown to be much more complex since it contributes to a number of catalytic functions [2]. In particular, it seems that ceria is involved in the formation and storage of sulphates due to sulphur impurities present in fuels. This sulphur originating from the gasoline as well as from the oil additives, reaches the catalysts mainly as SO₂ under normal operating conditions and has to be considered as a poisoning agent for the catalysts during oxidation reactions [3, 4]. In addition, cerium oxide is well-known to react with sulphur oxides over a wide range of temperature. Several types of sulphur species can be formed according to the oxidation state, the surface basicity and the sulphating conditions of ceria. Rodriguez *et al.* [5–7], have studied the reaction of SO₂ with pure and

---

*   Author for corespondence: E-mail: aboukais@univ-littoral.fr

reduced ceria by means of XANES, TPD and photoemission. A ceric sulphate $Ce(SO_4)_2$ phase has been evidenced on ceria surface at 100°C. In addition, it has been shown that the presence of oxygen vacancies in the CeO_2 favours the formation of SO_3 at the expense of SO_4. Otherwise, based on IR results, Waquif *et al.* [8–10] have proposed the formation of sulphite species on ceria surface by adsorption of SO_2 at room temperature. Heating of ceria in the presence of SO_2 gas at 100°C leads to the production of SO_4 species with a concomitant reduction of Ce(IV) to Ce(III). More importantly, formation of $Ce_2(SO_4)_3$ on ceria surface after adsorption of SO_2 or impregnation with $(NH_4)_2SO_4$ has been observed in the temperature range of 420–610°C by UV-visible [10], XPS [11, 12] and Raman spectroscopy [13].

In the present work, differently to results obtained in literature, cereous sulphate phase has been evidenced on ceria surface after adsorption of SO_2 at room temperature. Thermal analysis, Raman spectroscopy and EPR have been used in this study.

Experimental

Ceria was prepared by precipitation of cerium hydroxide from $Ce(NO_3)_3 \cdot 6H_2O$ with NaOH solution. The solid is calcined at 500°C for four hours under a flow of dried air 75 mL min^{-1}. The cooling period from 500°C to room temperature was about 2 h under the same air flow. The resulted ceria was treated in a micro-flow reactor under a flow of SO_2 gas (17 mL min^{-1}) at room temperature for 40 min. The $Ce(SO_4)_2 \cdot 4H_2O$ sample used as reference in this work is an Across product (purity>99%).

Thermal analysis of sulphated ceria and tetra-hydrated ceric sulphate $Ce(SO_4)_2 \cdot 4H_2O$ was performed using Netzsch STA 409 equipped with a micro-balance differential thermal analysis (DTA) and a flow gas system. α-Al_2O_3 was used as reference material. The sample was heated under air flow 75 mL min^{-1} from room temperature to 1000°C. The temperature was raised at a rate of 5°C min^{-1}.

Laser Raman spectra were recorded at room temperature using a Dilor XY monochromator with subtractive dispersion. The samples were excited using 632.8 nm radiation of He–Ne laser.

The EPR measurements were performed at –269°C on an EMX Bruker spectrometer with a cavity operating at a frequency of ~9.5 GHz (X band). The magnetic field was modulated at 100 kHz. The *g* values were determined from precise frequency and magnetic field values. The calculated spectra were simulated with Bruker 'SimFonia' program based upon perturbation theory [14].

Results and discussion

Thermal analysis study

Figure 1a illustrates the TG-DTA analysis obtained for ceria after treatment under a flow of SO_2 at room temperature. Two endothermic peaks appeared respectively at 160 and 785°C for sulphated ceria. The mass loss corresponding to the first endothermic peak can be attributed to the dehydration of the solid. Whereas, the 6.2% of mass

loss observed at 785°C is due to the decomposition of sulphate species, since no endothermic phenomenon was detected during the thermal decomposition of pure ceria between 250 and 800°C (Fig. 1b). The presence of only one endothermic peak at 785°C indicates that on the ceria surface there is the formation of only one type of sulphate species: $Ce(SO_4)_2$ or $Ce_2(SO_4)_3$. In order to elucidate which of these both compounds is responsible of this endothermic peak at 785°C; a ceric sulphate sample $[Ce(SO_4)_2 \cdot 4H_2O]$, was studied by TG-DTA analysis (Fig. 1c). Two endothermic peaks are observed at higher temperatures 500 and 840°C. Based on Yang and Rudong results [15], the former peak observed at 500°C can be attributed to the reduction of anhydrous ceric sulphate to cereous sulphate $Ce_2(SO_4)_3$, whereas the latter peak at 840°C can be assigned to the decomposition of cereous sulphate into CeO_2. The exothermic peak observed at 309°C can be attributed to a well crystallisation of the solid after dehydration since no simultaneous mass loss has been detected.
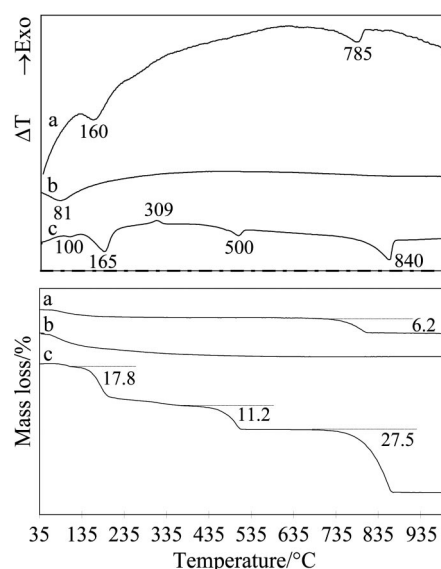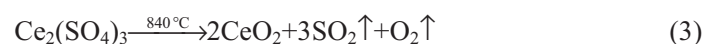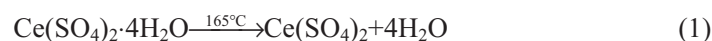

Fig. 1 Thermal analysis (TG-DTA) of a – sulphated ceria at 25°C; b – pure ceria and c – $Ce(SO_4)_2 \cdot 4H_2O$ sample at 25°C

On the basis of all these results, the thermal decomposition of tetra-hydrated ceric sulphate appears to proceed by the following stages:

$$Ce(SO_4)_2 \cdot 4H_2O \xrightarrow{165°C} Ce(SO_4)_2 + 4H_2O \qquad (1)$$

$$2Ce(SO_4)_2 \xrightarrow{500°C} Ce_2(SO_4)_3 + SO_2\uparrow + O_2\uparrow \qquad (2)$$

$$Ce_2(SO_4)_3 \xrightarrow{840°C} 2CeO_2 + 3SO_2\uparrow + O_2\uparrow \qquad (3)$$

The temperature range of each stage of $Ce(SO_4)_2 \cdot 4H_2O$ thermal decomposition associated with the calculated and observed mass loss are represented in Table 1.

Table 1 Temperature ranges and mass loss (%) observed and calculated for thermal decomposition of $Ce(SO_4)_2 \cdot 4H_2O$

T range/°C	Decomposition stage	Mass loss/%	
		experimental	theoretical
~165	loss of water molecules (1)	17.8	17.8
~500	reduction of Ce(IV) to Ce(III) (2)	11.2	11.6
~840	decomposition of $Ce_2(SO_4)_3$ (3)	27.5	27.7

The experimental mass losses have been calculated for 50 mg of tetrahydrated sulphated ceria $Ce(SO_4)_2 \cdot 4H_2O$ and the theoretical mass loss are calculated according to the reactions (1), (2) and (3). According to these results, the endothermic peak observed at 785°C after the thermal decomposition of sulphated ceria (Fig. 1a) can be compared to that obtained for $Ce_2(SO_4)_3$ at 840°C (Fig. 1c). This peak is then, due to the decomposition of cereous sulphate to CeO_2 through the reaction (3). The difference between the temperatures can be due to the fact that ceria can act as a catalyst favouring the decomposition of cereous sulphate at a lower temperature. Otherwise, in the difference to tetrahydrated ceric sulphate, no endothermic phenomenon has been observed in the temperature range between 450 and 500°C for sulphated ceria which has been attributed to the reduction of Ce(IV) to Ce(III)-sulphate. It can be deduced then, that only cereous sulphate species is formed upon interaction of ceria with sulphur dioxide SO_2 at room temperature. The formation of Ce(III)-sulphate can be interpreted by oxidation of SO_2 to sulphate species SO_4 with a concomitant reduction of Ce^{4+} to Ce^{3+} ions at room temperature. This reduction, leads to the formation of non-stoichiometric oxides CeO_{2-x} ($0<x<0.5$) associated with oxygen vacancies on ceria [16–18].

Only 6.2% of mass loss is observed for sulphated ceria at 785°C (Fig. 1a). However, the theoretical loss of cereous sulphate phase is about 39.4% (reaction (3)). This difference can be due to the fact that a large amount of ceria remains unchanged towards SO_2. Therefore, the resulted product obtained after treatment of ceria under SO_2 flow is composed by two phases: CeO_2 and $Ce_2(SO_4)_3$. The presence of these phases has been detected by Raman spectroscopy.

Raman study

Figure 2a, illustrates the Raman spectrum obtained after adsorption of SO_2 on the ceria sample at room temperature. This spectrum exhibits an intense band at 469 cm^{-1} associated with weak bands at 989, 1003, 1030 and 1126 cm^{-1}. These latters disappear while the calcination temperature of sulphated ceria reaches a temperature higher than 800°C (Fig. 2b). According to the literature data [19, 20], the strong band observed at 469 cm^{-1} was unambiguously assigned to F_{2g} mode characteristic of CeO_2. In fact, the Raman spectrum of pure ceria shows only the presence of the latter band (Fig. 2c). The other weak bands were attributed to S–O and S=O stretching vibrations of SO_4^{2-} species [21–23]. Indeed, it is known that Raman spectra of sulphate species exhibit bands between

965–1035 and 1100–1180 cm^{-1} due to symmetric and asymmetric SO stretching vibrations. However, no sulphite or disulphite species were detected on ceria surface since the characteristic Raman bands of these latters (950–975 and 1050–1100 cm^{-1}) [23–25] are absent from the spectrum (Fig. 2a). According to the thermal analysis (TG-DTA), these bands can be attributed only to the presence of cereous sulphate phase formed upon interaction of SO_2 with ceria at room temperature.
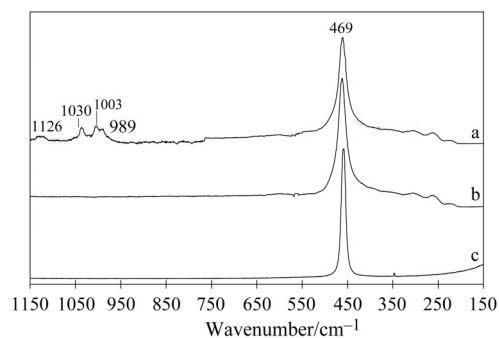

Fig. 2 Raman spectra of a – sulphated ceria at room temperature; b – sulphated ceria after treatment at 895°C and c – pure ceria

In addition, the Raman spectrum of sulphated ceria (Fig. 3a) is similar to that recorded for $Ce_2(SO_4)_3$ obtained after thermal treatment of ceric sulphate sample at 600°C (Fig. 3b). Whereas, it is different from that obtained for $Ce(SO_4)_2 \cdot 4H_2O$ at room temperature (Fig. 3c). Twu *et al.* [13] have obtained a similar Raman spectrum for $Ce_2(SO_4)_3$ sample at room temperature and for sulphated ceria heated at 450°C. Furthermore, this cereous sulphate phase $Ce_2(SO_4)_3$ has been proposed by XPS study

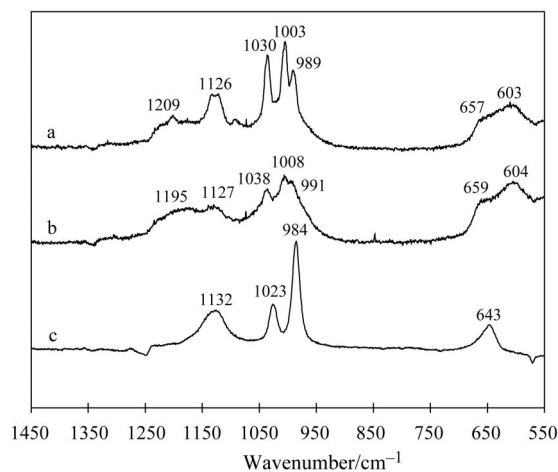**Fig 3** Raman spectra of a – sulphated ceria at 25°C; b – tetrahydrated ceric sulphate $Ce(SO_4)_2 \cdot 4H_2O$ treated at 600°C and c – tetrahydrated ceric sulphate at room temperature

of the oxidation states of cerium and sulphur for ceria treated with SO_2 at 550°C which has revealed the presence of Ce(III) and S(IV) [11, 12].

In conclusion, the interaction of ceria with SO_2 at room temperature leads only to the formation of $Ce_2(SO_4)_3$ loaded on ceria surface without any intermediate products such as ceric sulphite $Ce(SO_3)_2$ or ceric sulphate species $Ce(SO_4)_2$. Ceria, is the only product formed after the decomposition of $Ce_2(SO_4)_3$ species. The results of Raman spectroscopy are in perfect agreement with the thermal analysis observations and have evidenced the formation of cereous sulphate on ceria surface treated under SO_2 at room temperature. Furthermore, the difference between the experimental (6.2%) and theoretical (39.4%) mass loss of $Ce_2(SO_4)_3$ phase, can be explained by the fact that only 15.7% of ceria is transformed to $Ce_2(SO_4)_3$ after interaction with SO_2 at room temperature. The sample is then composed of 84.3% of pure ceria with 15.7% of $Ce_2(SO_4)_3$. Thus, the decomposition of sulphated ceria can be compared to the decomposition reaction (3) of $Ce_2(SO_4)_3$.

The change of oxidation state of Ce^{4+} to Ce^{3+} upon ceria sulphation at room temperature has been also evidenced by EPR study.

EPR Study

Figure 4 shows the EPR spectra obtained for pure ceria before and after treatment under SO_2 at room temperature with the EPR spectrum of tetrahydrated ceric sulphate treated at 600°C.

As shown in Fig. 4a, the EPR spectrum of sulphated ceria exhibits a complex superimposition of different signals. The first one characterized by $g_\perp=1.965$; $g_{//}=1.942$ and $g_{iso}=1.957$ has been widely investigated and attributed to the interaction between conduction electrons and 4f orbitals of Ce^{4+} ions in the CeO_2 matrix [16–18]. Moreover, these species are stabilised by oxygen defects in the CeO_2 matrix. The second centred at $g=2.013$ was attributed to O_2^- species [18]. The third obtained at $g=4.27$ is the well-known EPR transition for high spin Fe^{3+} ions; electronic configuration $(3d^5)$. Finally, a signal with weak intensity was observed at $g_\perp=0.57$; $g_{//}=3.97$; with $g_{iso}=1.70$. This signal is not observed for pure ceria before interaction with SO_2 at room temperature

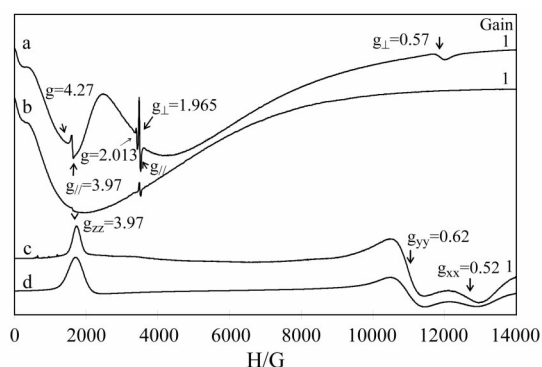**Fig. 4** EPR spectra of a – sulphated CeO_2 at 25°C; b – pure ceria; c – $Ce(SO_4)_2 \cdot 4H_2O$ sample treated at 600°C with d – the simulated spectrum

(Fig. 4b). In order to elucidate the attribution of this signal, and owing to the formation of $Ce_2(SO_4)_3$ phase after interaction of SO_2 with ceria at room temperature, the EPR signal of $Ce_2(SO_4)_3$ obtained after decomposition of $Ce(SO_4)_2 \cdot 4H_2O$ sample at 600°C was recorded (Fig.4c). An asymmetric EPR signal with $g_{zz}=3.97$; $g_{yy}=0.62$; $g_{xx}=0.52$ and $g_{iso}=1.70$ is then observed. The EPR parameters of this signal are confirmed by simulation (Fig. 4d) and are typical for the ions having the electronic $4f^1$ configuration. Based on the values of EPR parameters of this signal and according to the literature data [26, 27], this signal can be assigned to Ce^{3+} ions. In our case, the EPR signal observed for sulphated ceria at room temperature ($g_\perp=0.57$; $g_{//}=3.97$; $g_{iso}=1.70$) is similar to that obtained for $Ce_2(SO_4)_3$ (Fig. 4c). In fact, both signals have the same value of g_{iso} equal to 1.70. Thus, the EPR results provide evidence to the reduction of Ce^{4+} to Ce^{3+} after ceria sulphation. It can be deduced then that oxygen vacancies are present on the surface of sulphated ceria due to non-stoichiometric oxides CeO_{2-x} [16–18].

Based on these data, and the formation of oxygen vacancies after reduction of Ce^{4+} to Ce^{3+}, the following structure of cereous sulphate formed on ceria surface can be proposed:
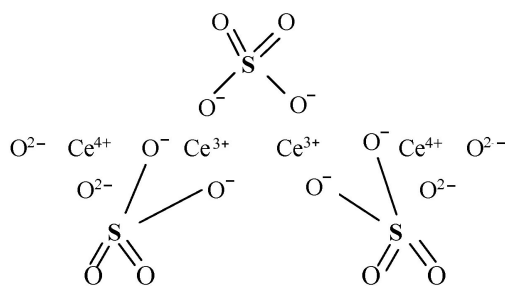
Scheme 1

Conclusions

This work has evidenced the strong affinity of cerium oxide surface towards sulphur dioxide. Upon treatment under SO_2 at room temperature ceria surface is easily sulphated into $Ce_2(SO_4)_3$. Ceria promotes the oxidation of SO_2 into SO_4 which is adsorbed as cereous sulphate at ceria surface. A concomitant reduction of Ce^{4+} to Ce^{3+} occurs during ceria sulphation. The formation of the Ce(III)-sulphate phase on ceria surface has been evidenced by thermal analysis, EPR and Raman spectroscopy. Cereous sulphate phase is completely decomposed at 785°C leading to the formation of CeO_2.

* * *

References

1 J. Yoo, A. Bhattacharyya, C. Radlowskiand and J. Karch, Appl. Catal. B., 1 (1992) 169.
2 B. Harrison, A. Diwell and C. Hallet, Platinum Metals Rev., 32 (1988) 73.
3 A. Trovarelli, Catal. Rev. Sci. Eng., 38 (1996) 439.
4 K. C. Taylor, Catal. Rev. Sci. Eng., 35 (1993) 457.
5 J. A. Rodriguez, T. Jirask, A. Fretag, J. C. Hanson, J. Z. Larese and S. Chatuverdi, Catal. Letters, 62 (1999) 113.
6 J. A. Rodriguez, T. Jirask, S. Chatuverdi and J. Hbreck, J. Am. Chem., 120 (1998) 11149.
7 S. Chatuverdi, J. A. Rodriguez, T. Jirask and J. Hrbeck, J. Phys. Chem. B., 102 (1998) 7033.
8 M. Waquif, A. Mohammed Saad, M. Bensitel, J. Bachelier, O. Saur and J. C. Lavalley, J. Chem. Soc. Faraday Trans., 88 (1992) 2931.
9 M. Waquif, P. Basin, O. Saur, J. C. Lavalley, G. Blanchard and O. Touret, Appl. Catal. B., 11 (1997) 193.
10 M. Waquif, Thèse, Caen, (1991).
11 D. D. Beck, M. H. Krueger and D. R Monroe, Society of Automotive Engineers, Inc., 910844 (1991).
12 A. F. Diwell, C. Halett and J. R. Taylor, Society of Automotive Engineers, Inc., 872163 (1987).
13 J. Twu, J. C. Chuang, K. Chang, Y. C. Hsiang and K. H. Chen, Appl. Catal. B: Environmental, 12 (1997) 309.
14 R. T. Weber, WINEPR SIMFONIA manuel, Ver 1.2, Brucker Instruments, Inc., Billerica, Ma and references therein, 1995.
15 Y. Yang and Y. Rudong, Thermochim. Acta, 202 (1992) 301.
16 E. Abi-Aad, A. Bennani, J. P. Bonnelle and A. Aboukaïs, J. Chem. Soc., Faraday Trans., 91 (1995) 99.
17 A. Aboukaïs, A. Bennani, C. F. Aïssi, G. Wrobel, M. Guelton and J. C. Vedrine, J. Chem. Soc., Faraday Trans., 88 (1992) 615.
18 E. Abi-Aad, R. Bechara, J. Grimblot and A. Aboukaïs, Chemistry of Materials, 5 (1993) 793.
19 P. Fornasiero, G. Balducci, R. Di Monte, J. Kaspar, V. Sergo, G. Gubitosa, A. Ferrero and M. Graziani, J. Catal., 164 (1995) 173.
20 N. Sergent, J. F. Lamonier and A. Aboukaïs, Chem. Mater., 12 (2000) 3830.
21 W. H. Weber, K. C. Hass and J. R. McBride, Phys. Rev. B., 48 (1993) 178.
22 J. Z. Shyu, W. H. Weber and H. S. Gandhi, J. Phys. Chem., 92 (1988) 4964.
23 I. A. Degen and G. A. Newman, Spectrochim. Acta, Part A., 49A (1993) 859.
24 V. P. Verma, Thermochim. Acta, 89 (1985) 363.
25 S. Sato, S. Highuchi and S. Tanaka, Appl. Spectrosc., 39 (1985) 822.
26 D. L Griscom, Journal of Non-Crystalide Solid, 40 (1980) 211.
27 E. Abi-Aad, E. Zhilinskaya and A. Aboukaïs, J. Chim. Phys., 96 (1999) 1519.